Quantum Electronics **40** (10) 879–886 (2010)

OPTICAL FIBRES

PACS numbers: 07.60.Vg; 42.79.Fm; 42.81.Wg
DOI: 10.1070/QE2010v040n10ABEH014385

Reversible changes in the reflectivity of different types of fibre Bragg gratings

P.I. Gnusin, S.A. Vasil'ev, O.I. Medvedkov, E.M. Dianov

***Abstract*. We have studied strain- and temperature-induced reversible changes in the reflectivity of different types of fibre Bragg gratings. The results demonstrate that the strain sensitivity of the reflectivity of type I and IIa Bragg gratings is mainly due to the photoinduced reduction in the elasto-optic coefficient p_{12} of the core glass and that its temperature sensitivity results from the increase in the thermo-optic coefficient of the glass. UV exposure of fibres loaded with molecular hydrogen has an insignificant effect on these material coefficients. We also analyse the effects of UV fluence and germanium concentration in the fibre core on the reversible changes in the reflectivity of the grating.**

Keywords: *fibre Bragg grating, reflectivity, temperature and strain effects.*

1. Introduction

Photoinduced fibre Bragg gratings (FBGs) are widely used in a variety of fibreoptic applications, such as communication systems, fibre lasers and sensors [1, 2]. Even though the application field of FBGs is continuously expanding, the physical mechanisms of photoinduced refractive index changes, underlying the possibility of producing index gratings, are still unclear in many aspects, even for the most widespread, germanium-doped fibre.

Germanosilicate fibres are known to exhibit several types of photosensitivity, depending on fabrication conditions, grating inscription and annealing dynamics and other properties of photoinduced FBGs (see Vasil'ev et al. [3] and references therein). The type of an FBG is determined by the dominant type of photosensitivity in it. Type I photosensitivity is characterised by a monotonic increase in the refractive index of the core glass during UV exposure. During FBG inscription into high-GeO_2 fibre, the photoinduced index modulation amplitude varies nonmonotonically. This is caused by type IIa photosensitivity, which makes a negative contribution to the photoinduced index change. Laser pulses with a high energy density (above 1 J cm^{-2}) cause local melting of the core glass, leading to the formation of type II FBGs. After low-temperature hydrogen loading, fibres exhibit type I(H_2) photosensitivity, which ensures index changes about an order of magnitude greater than those in the type I gratings. Type Ia photosensitivity is observed in hydrogen-loaded germanium-boron codoped fibres at high UV fluences.

The main spectral characteristics of a uniform FBG (i.e. an FBG with a constant index modulation amplitude and period) are the resonance wavelength, λ_{Br}, and the reflectivity at this wavelength, R_{Br}. The resonance wavelength of an FBG in the first diffraction order is given by

$$\lambda_{Br} = 2n_{eff}\Lambda, \tag{1}$$

where n_{eff} is the effective refractive index of the fundamental mode after the UV exposure and Λ is the grating period. The reflectivity of a uniform FBG at the resonance wavelength is a function of the FBG length, L, and the coupling coefficient, k:

$$R_{Br} = \tanh^2(kL). \tag{2}$$

Here $k = \pi\eta\Delta n_{mod}/\lambda_{Br}$ is the coupling coefficient per unit FBG length, where Δn_{mod} is the index modulation amplitude in the first diffraction order and η is the fractional power of the fundamental mode in the fibre core (as a rule, photoinduced index changes occur in the core glass, which has an appreciable absorption coefficient at the writing wavelength).

The λ_{Br} and R_{Br} values are sensitive to external influences (temperature, strain, UV exposure and others) capable of changing the refractive index of the glass or the FBG period. Changes λ_{Br} and R_{Br} may be both reversible (the initial value is restored after the perturbations are eliminated) and irreversible. Irreversible changes in FBG parameters occur, e.g., when the grating is heated to a temperature high enough to anneal out the photoinduced index change [4] or when it is exposed to UV radiation that influences the refractive index of the fibre core. The latter is used to inscribe gratings and to modify their spectral characteristics by UV exposure.

Analysis of reversible changes in FBG parameters usually deals with λ_{Br} changes, which allow one to produce tunable spectral filters [5] and sensors [6].

P.I. Gnusin, S.A. Vasil'ev, O.I. Medvedkov, E.M. Dianov Fiber Optics Research Center, Russian Academy of Sciences, ul. Vavilova 38, 119333 Moscow, Russia; e-mail: sav@fo.gpi.ru

Received 25 June 2010
Kvantovaya Elektronika **40** (10) 879–886 (2010)
Translated by O.M. Tsarev

The temperature coefficient of the resonance wavelength of an FBG is given by

$$K_T = \frac{1}{\lambda_{Br}}\frac{d\lambda_{Br}}{dT} = \frac{1}{n_{eff}}\frac{dn_{eff}}{dT} + \alpha, \quad (3)$$

where α is the thermal expansion coefficient of silica glass. Because of the low thermal expansion coefficient of silica, the main contribution ($\sim 95\,\%$) to λ_{Br} changes comes from its thermo-optic coefficient, dn/dT [6]. FBGs range fairly widely in K_T , depending on the type of photosensitivity. In particular, as shown by Shu et al. [7] for germanium-boron codoped fibres, the highest thermal sensitivity in the temperature range $0-80\,^{\circ}C$ is offered by type IIa FBGs [$K_T \sim (6.4-6.9)\times 10^{-6}$ K^{-1}], and the lowest, by type Ia FBGs [$K_T \sim (4.5-5.1)\times 10^{-6}$ K^{-1}].

The strain response of λ_{Br} is given by

$$K_\varepsilon = \frac{1}{\lambda_{Br}}\frac{d\lambda_{Br}}{d\varepsilon} = 1 - \frac{n_{eff}^2}{2}p, \quad (4)$$

here ε is tensile strain and

$$p = [p_{12} - \nu(p_{11} + p_{12})], \quad (5)$$

where p_{11} and p_{12} are the Pockels (elasto-optic) coefficients and ν is the Poisson's ratio of silica glass. The main contribution to K_ε comes from changes in FBG period, whereas the index change due to the elasto-optic effect is comparatively small ($\sim 22\,\%$) [6]. This probably accounts for the fact that K_ε varies little from one type of FBG to another ($\sim 1\,\%$) [7].

Reversible changes in the reflectivity of FBGs R_{Br} have been studied in much less detail. As shown by Hidayat et al. [8], with increasing temperature the R_{Br} of type I gratings increases, whereas that of type IIa FBGs decreases. It is remarkable that the reflectivity of type I(H_2) gratings, written after low-temperature loading with molecular hydrogen, is essentially temperature-independent. R_{Br} changes in unloaded FBGs were attributed to UV-induced changes in the thermal expansion coefficient, which depends on the type of photosensitivity. According to Hidayat et al. [8], UV exposure reduces the thermal expansion coefficient of the germanosilicate core glass in type I FBGs and increases it in type IIa FBGs.

Akulov et al. [9] and Vlasov [10] investigated axial-strain-induced reversible changes in the reflectivity of FBGs. The observed considerable (factor of 1.5) increase in index modulation amplitude upon a 5 % FBG compression was attributed to the photoinduced increase (by about 1 %) in the elasto-optic coefficient of the fibre core material.

In this paper, we present new data on temperature- and strain-induced reversible changes in index modulation amplitude in type I, IIa and I(H_2) FBGs.

2. Experimental procedure

FBGs for this investigation were written in single-mode fibres whose main parameters are listed in Table 1. All the fibres except fibre A (standard telecom fibre SMF-28) were fabricated at the Fiber Optics Research Center, Russian Academy of Sciences (RAS), from MCVD preforms produced at the Institute of Chemistry of High-Purity Substances, RAS. The fibres were doped with germanium to different concentrations and contained no other dopants.

Table 1. Parameters of optical fibres (λ_c is the first higher order mode cutoff wavelength and Δ is the relative core–cladding index difference).

Fibre	mol % GeO_2	Δ	λ_c/nm
A	3.5	0.0038	1250
B	5	0.0055	960
C	14.5	0.0124	1010
D	24	0.0234	980
E	33	0.0315	1200

The gratings were written using a frequency-doubled cw Ar^+ laser ($\lambda = 244$ nm) and Lloyd interferometer [11]. During the FBG inscription, the average UV power density was ~ 40 W cm^{-2} and the interference fringe contrast was close to unity. The resonance wavelengths of the FBGs employed in our experiments were in the range 1550 ± 10 nm. The grating length in unloaded fibres was 3–4 mm, and that in H_2-loaded fibres (100 atm, 20 h, 100 °C) was just 1–2 mm.

After the inscription process, the FBGs were heat-treated in a furnace at 150 °C for 10 h in order to remove the residual molecular hydrogen in the case of the type I(H_2) FBGs and also to rule out the effect of the unstable component of the photoinduced index change on its temperature behaviour.

3. Strain-induced reversible changes in the reflectivity of FBGs

Axial tensile strain in the fibre section containing an FBG was produced using two 40-mm-diameter cylinders. Several fibre turns were secured around both cylinders, and a tensile load was produced by applying a torque to one of them. The strain suffered by the FBG was evaluated from the measured λ_{Br} using (4) with $K_\varepsilon = 0.787$.

We measured the resonance wavelength, λ_{Br}, and transmittance at this wavelength, T_{Br}, as functions of strain. Transmission spectra were taken on an Ando AQ6317 optical spectrum analyser at a spectral resolution of 0.02 nm, using depolarised radiation from a broadband erbium-doped fibre source. The λ_{Br} and T_{Br} values were determined from experimental data with an accuracy of 0.01 nm and 0.5 %, respectively. The reflectivity of the FBGs was determined as $R_{Br} = 1 - T_{Br}$.

Figure 1 shows the room-temperature transmission spectra of the three types of FBGs written in fibre E. The spectra were measured at zero strain and a tensile strain of 5000 $\mu\varepsilon$ ($\mu\varepsilon$ is a relative elongation of 10^{-6}). Stretching increased the reflectivity of the type I FBG from 46.5 % to 50.7 % (Fig. 1a), whereas the same strain reduced the R_{Br} of the type IIa FBG from 51.3 % to 46.2 % (Fig. 1b). The reflectivity of the FBG written after hydrogen loading changed only slightly, by $-0.5\,\%$ (Fig. 1c).

To our knowledge, such considerable strain-induced changes in reflectivity and opposite signs of the effects in type I and IIa FBGs were observed for the first time. These effects should be taken into account in practical applications of such FBGs where their reflectivity is critical. For example, this may be important in designing tunable FBG filters, fibre lasers with an output wavelength tunable by applying strain to an FBG and fibre sensors of physical variables that measure the intensity reflected from a strained FBG.

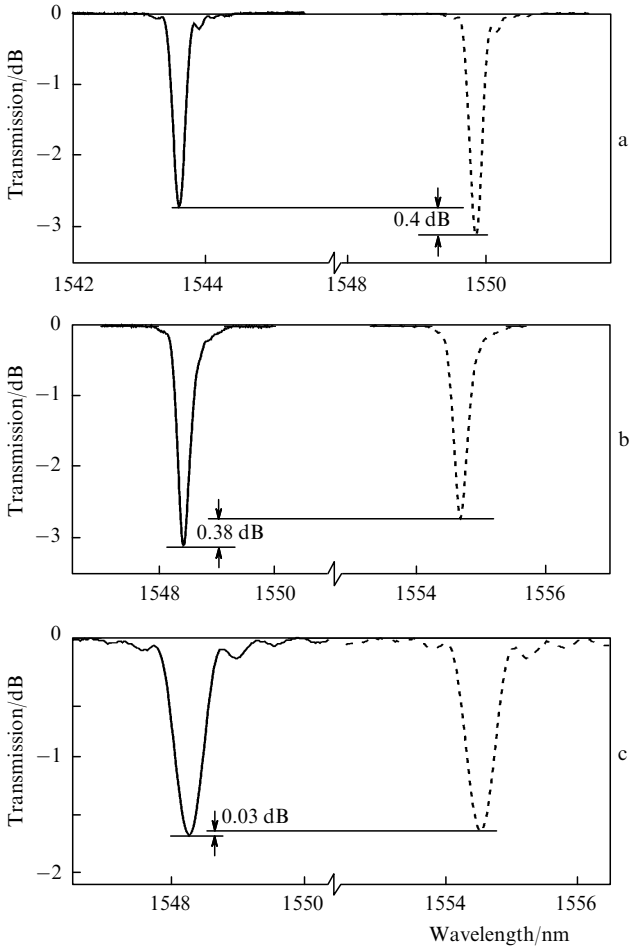

Figure 1. Transmission spectra of type (a) I, (b) IIa and (c) I(H_2) FBGs at zero strain (solid lines) and a tensile strain of 5000 $\mu\varepsilon$ (dashed lines).

When the photoinduced index change, $\Delta n_{\mathrm{ind}}(D)$, is a nonlinear function of UV fluence, typical of fibre grating inscription into germanosilicate fibres, the axial index profile, $\Delta n_{\mathrm{ind}}(z)$, in a uniform FBG can be represented by the Fourier series

$$\Delta n_{\mathrm{ind}}(z) = \overline{\Delta n} + \sum_{m=1}^{\infty} A_m \cos\left(\frac{2\pi m}{\Lambda} z\right), \tag{6}$$

where $\overline{\Delta n}$ is the average photoinduced index change in the fibre core and m is the diffraction order. We assume here that the axial UV intensity profile has the form

$$I(z) = \frac{I_{\max}}{2}\left[1 + \cos\left(\frac{2\pi}{\Lambda} z\right)\right], \tag{7}$$

where $I_{\max}$ is the UV intensity at the crests of the interference pattern.

The $m = 1$ alternating coefficient in series (6) (it is the first diffraction order which is employed in most cases, including this study) is generally related to Δn_{mod} by $|A_1| = \Delta n_{\mathrm{mod}}$, with $A_1 > 0$ for type I and I(H_2) FBGs and $A_1 < 0$ for type IIa.

The FBG length varies with temperature and strain, whereas the number of grating lines, N, remains unchanged. Therefore, to analyse the temperature and strain effects on the reflectivity of different types of FBGs, it is convenient to introduce a nondimensional alternating coupling parameter of FBGs:

$$\Omega = \frac{\pi \eta A_1}{2 n_{\mathrm{eff}}}. \tag{8}$$

Its magnitude is equal to the coupling coefficient per grating line. The reflectivity of the grating is related to this parameter by

$$R_{\mathrm{Br}} = \tanh^2(|\Omega| N). \tag{9}$$

We think that the observed strain effects on the R_{Br} of the type I and IIa gratings (Fig. 1) are of the same physical nature and that they have opposite signs because the photoinduced index change is positive in the type I FBGs and negative in the type IIa FBGs [12]. It is the commonness of the phenomenon under investigation that led us to introduce a special parameter, Ω, whose reversible change $\Delta\Omega$ has the same (positive) sign in the above types of gratings.

Figure 2 shows the relative change in Ω as a function of strain for the FBGs represented in Fig. 1 (Ω_0 is the coupling parameter at the initial FBG temperature and zero strain). The experimental data are seen to be well fitted by straight lines, which attests to linear behaviour of the reversible index change in all the grating types throughout the strain range studied. In particular, the slope $(1/\Omega_0)(\mathrm{d}\Omega/\mathrm{d}\varepsilon)$ is $(0.135 \pm 0.005) \times 10^{-4} \mu\varepsilon^{-1}$ [$\Omega_0 = (1.13 \pm 0.02) \times 10^{-4}$] for the type I FBG, $(0.128 \pm 0.005) \times 10^{-4}\ \mu\varepsilon^{-1}$ [$\Omega_0 = (-1.43 \pm 0.02) \times 10^{-4}$] for the type IIa FBG, and $(-0.016 \pm 0.005) \times 10^{-4}\ \mu\varepsilon^{-1}$ [$\Omega_0 = (2.00 \pm 0.03) \times 10^{-4}$] for the type I($H_2$) FBG.

The strain sensitivity of Ω can be represented as the sum of contributions from different physical mechanisms:

$$\frac{\mathrm{d}\Omega}{\mathrm{d}\varepsilon} = \left(\frac{\mathrm{d}\Omega}{\mathrm{d}\varepsilon}\right)_{\mathrm{W}} + \left(\frac{\mathrm{d}\Omega}{\mathrm{d}\varepsilon}\right)_{\mathrm{S}} + \left(\frac{\mathrm{d}\Omega}{\mathrm{d}\varepsilon}\right)_{\mathrm{Ph}}. \tag{10}$$

The first term on the right-hand side of (10) represents the strain effect on Ω through changes in the guidance

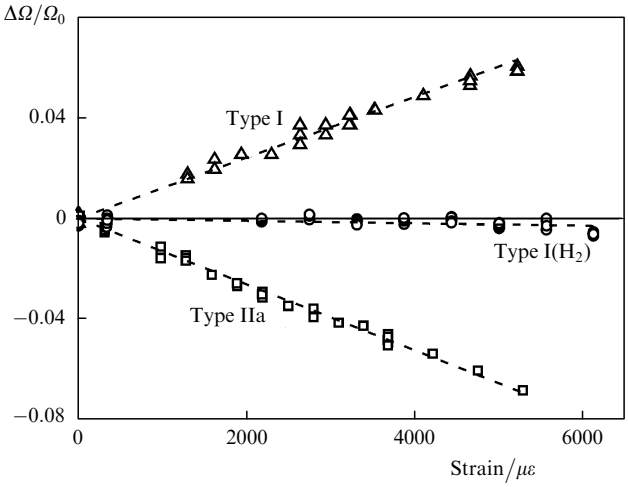

Figure 2. Relative change in Ω as a function of strain for different types of FBGs.

characteristics of the fibre and is unrelated to the parameters of the grating. The second term describes the contribution of the change in index modulation amplitude Δn_{mod}, under the assumption that the elastic and elasto-optic constants of the glass are unaffected by the UV exposure. Finally, the third term arises from the contribution to Δn_{mod} from the photoinduced changes in the above parameters of the core glass.

To assess the contributions of the different terms in (10), we represent the FBG as consisting of alternating (irradiated and unirradiated) regions, each of length $\Lambda/2$, with a constant UV fluence within each irradiated region. In considering the strain in the irradiated and unirradiated regions of the core, we neglect the influence of the fibre cladding. The first two terms in (10) can then be represented in the form

$$\frac{1}{\Omega_0}\left[\left(\frac{\mathrm{d}\Omega}{\mathrm{d}\varepsilon}\right)_{\mathrm{W}}+\left(\frac{\mathrm{d}\Omega}{\mathrm{d}\varepsilon}\right)_{\mathrm{S}}\right]\approx-\frac{2+2v+V^2n_{\mathrm{eff}}^2p}{V^2-1}, \qquad (11)$$

where V is the normalised frequency at the resonance wavelength of the FBG.

Using the v and p of silica glass [13], we find that, for fibre E, the right-hand side of (11) is $-0.016\times10^{-4}\ \mu\varepsilon^{-1}$, in perfect agreement with the strain sensitivity of Ω for the type I(H_2) FBGs (Fig. 2). Therefore, the strain effect on the reflectivity of the type I(H_2) FBGs is dominated by the first two terms in (10), which means that the inscription of this type of FBG causes no significant changes in the parameters of the core glass. To further validate this conclusion, we tested two FBGs written in the same fibre at higher UV fluences. Figure 3 plots $\mathrm{d}\Omega/\mathrm{d}\varepsilon$ against Ω for the three type I(H_2) FBGs. The data are well fitted by a straight line passing through the origin. Its slope ($-0.0155\times10^{-4}\mu\varepsilon^{-1}$) also agrees well with that estimated from (11).

In contrast, the strain response of the type I and IIa FBGs differs markedly from the estimated one (Fig. 2), suggesting that UV exposure influences parameters of the core glass. Under the above assumptions, the third term on the right-hand side of (10) can be written in the form

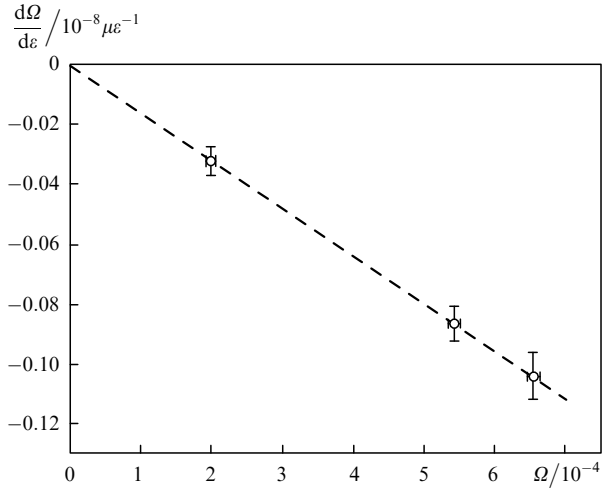

Figure 3. $\mathrm{d}\Omega/\mathrm{d}\varepsilon$ as a function of Ω for type I(H_2) FBGs.

$$\left(\frac{\mathrm{d}\Omega}{\mathrm{d}\varepsilon}\right)_{\mathrm{Ph}}\approx\frac{\pi\eta}{2}p\left(\frac{\delta E}{E}-\frac{\delta p}{p}\right), \qquad (12)$$

where δE and δp are the photoinduced changes in Young's modulus (E) and p, respectively.

Equation (12) suggests that the observed strain-induced increase in the Ω of the type I and IIa FBGs might be due to a photoinduced increase in Young's modulus or decrease in p. An important point is that such behaviours of E and p ($\delta E>0$, $\delta p<0$) should persist at fluences corresponding to the two types of FBGs. In particular, as found by Aashira et al. [14], pulsed UV irradiation of bulk glass samples containing ~10 mol% GeO_2 leads to a considerable, nonmonotonic variation in their Young's modulus (with a maximum in E). Such nonmonotonic behaviour of δE cannot account for the present data.

We assume that the strain effect on Ω and, as a consequence, on R_{Br} is mainly due to the photoinduced reduction in p. Note that this coefficient is determined primarily by the transverse component of the elasto-optic tensor, p_{12}, as seen from (5). In particular, the above results for the type I and IIa FBGs can be accounted for by a 1% photoinduced decrease in p_{12} at constant E. It follows from relation (4) that such a small change in elasto-optic coefficient cannot produce any marked change in $\mathrm{d}\lambda_{\mathrm{Br}}/\mathrm{d}\varepsilon$, in accordance with earlier experimental data, e.g. those of Shu et al. [7].

4. Temperature-induced reversible changes in the reflectivity of FBGs

To study temperature-induced reversible changes in the reflectivity of FBGs, we used an automatic system described elsewhere [15]. An unstrained FBG was placed in a furnace and heated from 25 to 145 °C at a constant rate of 0.1 °C s^{-1}. During heating, the transmission spectrum of the FBG was measured at intervals. The time taken to measure the spectrum was ~12 s.

Figure 4 shows the transmission spectra of the type I, IIa and I(H_2) FBGs at 25 °C and an elevated temperature. It is remarkable that the temperature effect on R_{Br} was similar to the effect of tensile strain (Fig. 1). In particular, the above heating increased the reflectivity of the type I FBG by 3.1% and reduced that of the type IIa FBG by 3.0%. The reflectivity of the type I(H_2) FBG remained unchanged to within the measurement accuracy.

Figure 5 illustrates the temperature effect on the coupling parameter Ω of the FBGs. As in the case of the strain response, Ω is a linear function of temperature for the three grating types. The slope $(1/\Omega_0)(\mathrm{d}\Omega/\mathrm{d}T)$ is $(6.6\pm0.2)\times10^{-4}\ \mathrm{K}^{-1}$ for the type I FBG, $(6.1\pm0.2)\times10^{-4}\ \mathrm{K}^{-1}$ for the type IIa FBG and below $10^{-5}\ \mathrm{K}^{-1}$ (measurement uncertainty) for the type I(H_2) FBG. Note that the present results agree well with earlier data [8].

By analogy with (10), $\mathrm{d}\Omega/\mathrm{d}T$ can be represented as the sum of contributions from different temperature-induced processes:

$$\frac{\mathrm{d}\Omega}{\mathrm{d}T}=\left(\frac{\mathrm{d}\Omega}{\mathrm{d}T}\right)_{\mathrm{W}}+\left(\frac{\mathrm{d}\Omega}{\mathrm{d}T}\right)_{\mathrm{T}}+\left(\frac{\mathrm{d}\Omega}{\mathrm{d}T}\right)_{\mathrm{Ph}}. \qquad (13)$$

Like in (10), the subscript W marks the term that represents the temperature variation of the parameters of the fibre. The second term in (13) describes the temperature variation

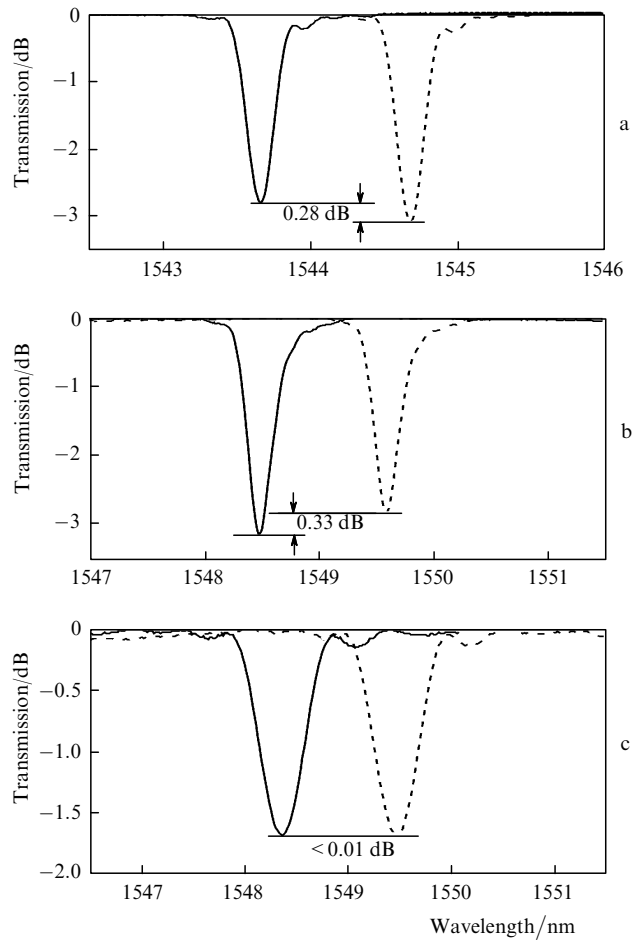

Figure 4. Transmission spectra of type (a) I, (b) IIa and (c) I(H_2) FBGs at 25 (solid lines) and 125 °C (dashed lines).

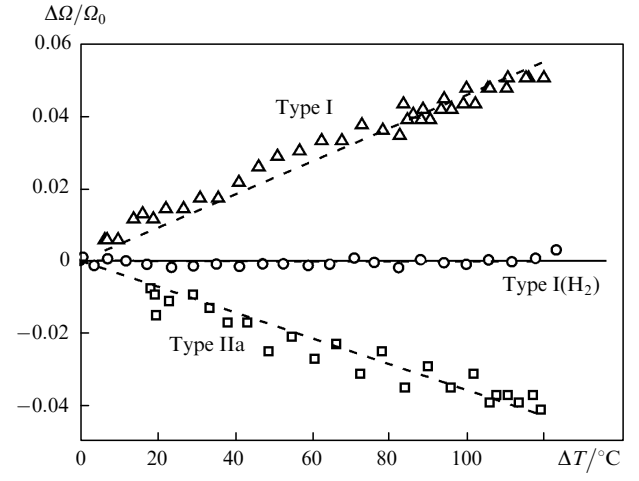

Figure 5. Relative change in Ω as a function of temperature change for different types of FBGs.

of Δn_{mod} under the assumption that the parameters of the glass are unaffected by the UV exposure. This term is due to changes in index modulation amplitude through the thermo-optic effect and also to the thermal stress in the fibre core, which leads to different index changes in the irradiated and unirradiated regions of the core. Finally, the third term in (13) describes the contribution to Δn_{mod} from the photoinduced changes in the material parameters of the fibre core that are responsible for the temperature effect on the properties of the glass.

Under the assumptions made in deriving relation (11), the first two terms in Eqn (13) have the form

$$\frac{1}{\Omega_0}\left[\left(\frac{d\Omega}{dT}\right)_W + \left(\frac{d\Omega}{dT}\right)_T\right] \approx -\frac{1}{n_{eff}}\frac{dn_{eff}}{dT}\frac{V^2}{V^2-1} + 3p(\alpha_{co}-\alpha_{cl}), \quad (14)$$

where α_{co} and α_{cl} are the thermal expansion coefficients of the core and cladding, respectively.

Using the thermal expansion coefficient vs. GeO_2 concentration data [8], we obtain from (14) for an FBG in fibre E $(1/\Omega_0)(d\Omega/dT) \approx -5.6\times10^{-6}$ K^{-1}, which lies within the accuracy limits of our experiments (10^{-1} K^{-1}). This explains why the Ω of the type I(H_2) FBGs did not vary with temperature and suggests that the inscription of such gratings did not influence any parameters of the glass. At the same time, the markedly larger $d\Omega/dT$ values for the type I and IIa FBGs (Fig. 5) indicate that the UV exposure of the hydrogen-free fibre influenced the physical properties and performance parameters of the glass.

The contribution of photoinduced changes in material parameters to $d\Omega/dT$ can be represented in the form

$$\left(\frac{d\Omega}{dT}\right)_{Ph} \approx \frac{\pi\eta}{2}\left[\delta\left(\frac{1}{n_{eff}}\frac{dn_{eff}}{dT}\right) - \left(\alpha_{co}-\alpha_{cl}+\frac{\delta\alpha_{co}}{2}\right)\left(\frac{\delta E}{E}-\frac{\delta p}{p}\right)p\right]. \quad (15)$$

As above, δ refers to UV-induced changes in material parameters.

Because silica and germanosilicate glasses have a low thermal expansion coefficient, the second term in square brackets is small compared to the first. Given this, we assume that $d\Omega/dT$ is determined primarily by the photoinduced change in the thermo-optic coefficient of the core glass, rather than by the photoinduced change in the thermal expansion coefficient, in contrast to what was assumed by Hidayat et al. [8]. To explain the data for the type I and IIa FBGs in Fig. 5, it is reasonable to assume that the writing of these FBGs was accompanied by a photoinduced increase in the thermo-optic coefficient by about 1.2 %.

Note that, since $\delta(n_{eff}^{-1}(dn_{eff}/dT))$ depends on the type of FBG photosensitivity, it follows from (3) that, as mentioned above, the different types of FBGs differ in $d\lambda_{Br}/dT$. Because our results demonstrate that $\delta(n_{eff}^{-1}(dn_{eff}/dT)) \approx 0$ for the type I(H_2) FBGs and $\delta(n_{eff}^{-1}(dn_{eff}/dT)) > 0$ for the type I and IIa FBGs, the temperature sensitivity of the wavelength in the type I(H_2) gratings should be lower than that in the hydrogen-free FBGs, as was observed by Shu et al. [7]. The thermo-optic coefficients calculated from their data for the type I(H_2) and IIa FBGs differ by about 5 %–10 %. This markedly exceeds our estimate, $\delta(n_{eff}^{-1}(dn_{eff}/dT)) \sim 1.2$ %, of the photoinduced change in the thermo-optic coefficient in $d\Omega/dT$ calculation. The origin of the discrepancy requires further investigation, but it is reasonable to assume that it is the consequence of the comparatively rapid saturation of $\delta(n_{eff}^{-1}(dn_{eff}/dT))$ with increasing UU fluence, which may influence FBG

inscription even at a relatively high interference fringe contrast.

5. Effects of UV fluence and germanium concentration in the fibre core on reversible changes in Ω

As shown above, reversible changes in the coupling parameter Ω in hydrogen-free germanosilicate fibres are due to photoinduced changes in parameters of the glass, which should depend on UV fluence.

Figure 6 plots Ω against fluence for fibre E. The data can be understood in terms of a model that considers three states (energy levels) of the glass network [12, 16]. The model assumes that, in the initial state, the glass network is in state 1 with population N. UV exposure causes transitions of the glass network from state 1 to state 2 and then from state 2 to state 3. The transition to state 2 corresponds to an increase in the refractive index (type I photosensitivity), and that to state 3 corresponds to a decrease in the refractive index (type IIa photosensitivity).

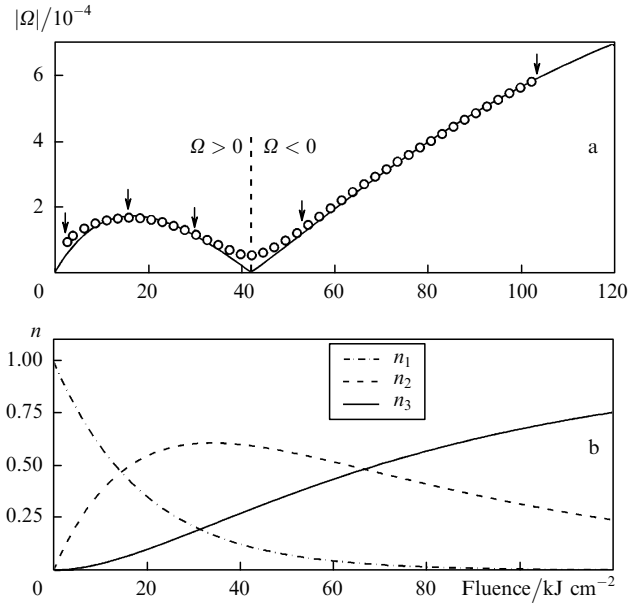

Figure 6. (a) Measured (open circles) and calculated (solid line) Ω as a function of average UV fluence and (b) relative level populations calculated in the model of Dong et al. [12]. The arrows mark the UV fluences used to inscribe five FBGs.

The model gives the following expressions for the relative populations of the three states, n_1, n_2, n_3 as functions of exposure time, t:

$$
\begin{aligned}
n_1 &= \exp(-B_{12}It),\\
n_2 &= \frac{B_{12}}{(B_{12}-B_{23})}[\exp(-B_{23}It)-\exp(-B_{12}It)],\\
n_3 &= 1-\frac{B_{12}}{(B_{12}-B_{23})}\exp(-B_{23}It)\\
&\quad+\frac{B_{23}}{(B_{12}-B_{23})}\exp(-B_{12}It),
\end{aligned}
\tag{16}
$$

where I is the UV intensity at the crests of the interference pattern, and B_{12} and B_{23} characterise the rates of the respective transitions. The sum of the relative populations is constant at unity.

The photoinduced index change is given by

$$\Delta n_{\mathrm{ind}} = (n_2S_2 + n_3S_3)N, \tag{17}$$

where S_2 and S_3 characterise the index change per unit population of levels 2 and 3, respectively.

The best fit to the experimental data in this model was obtained with $S_2N = 1.28\times10^{-3}$, $S_3N = -2.3\times10^{-3}$, $(B_{12})^{-1} = 38.5$ kJ cm^{-2}, $(B_{23})^{-1} = 138$ kJ cm^{-2} and $I_{\max} = 80$ W cm^{-2} (Fig. 6a, solid line). Figure 6b shows the relative level populations n_1, n_2 and n_3 in model (16) as functions of average UV fluence.

To examine $\mathrm{d}\Omega/\mathrm{d}\varepsilon$ and $\mathrm{d}\Omega/\mathrm{d}T$ as functions of UV fluence in fibre E with no hydrogen loading, we used five FBGs written with fluences of 1.7, 15, 30, 55 and 105 kJ cm^{-2} (marked by arrows in Fig. 6a). Figure 7 illustrates the temperature and strain effects on Ω for these FBGs. As pointed out above, heating and strain increase this parameter in both the type I ($D < 42$ kJ cm^{-2}) and type IIa ($D > 42$ kJ cm^{-2}) FBGs, which indicates that the refractive index in the exposed regions of the FBGs increases (on both stretching and heating) relative to that of the unexposed regions and that this behaviour is independent of the grating type.

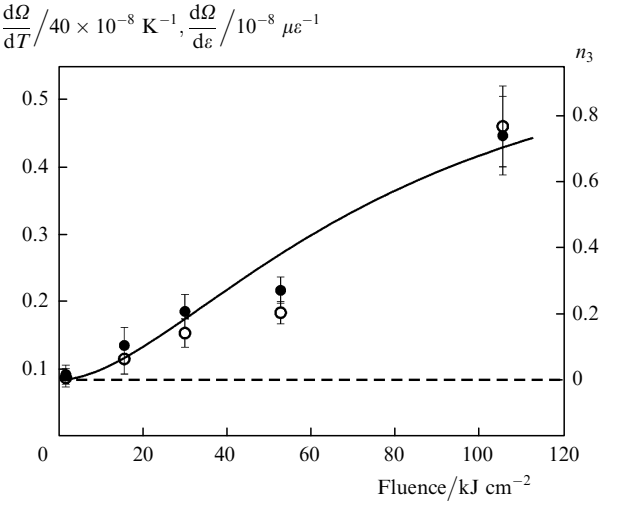

Figure 7. $\mathrm{d}\Omega/\mathrm{d}\varepsilon$ (○) and $\mathrm{d}\Omega/\mathrm{d}T$ (●) as functions of UV fluence for type I and IIa FBGs written in fibre E and the population of level 3 (solid line). The dashed line shows $\mathrm{d}\Omega/\mathrm{d}\varepsilon$ and $\mathrm{d}\Omega/\mathrm{d}T$ at low fluence.

As seen in Fig. 7, both $\mathrm{d}\Omega/\mathrm{d}\varepsilon$ and $\mathrm{d}\Omega/\mathrm{d}T$ increase monotonically with UV fluence, and the data points for these quantities almost coincide (on the scales used in Fig. 7). This indicates that the physical mechanisms responsible for the observed reversible changes in Ω have a general character.

The quantities $\mathrm{d}\Omega/\mathrm{d}\varepsilon$ and $\mathrm{d}\Omega/\mathrm{d}T$ differ from zero even at low fluences (the level marked by a dashed line). The $(\mathrm{d}\Omega/\mathrm{d}\varepsilon)^0$ and $(\mathrm{d}\Omega/\mathrm{d}T)^0$ of the FBG written at the lowest fluence (1.7 kJ cm^{-2}) are $\sim0.09\times10^{-8}$ $\mu\varepsilon^{-1}$ and $\sim3.6\times10^{-8}$ K^{-1}, respectively. This means that, at the very beginning of exposure (fluences within 1 kJ cm^{-2}), these

quantities in the exposed regions of the fibre core vary rather rapidly. Note that, at low UV fluences both in continuous and pulsed modes, the refractive index rises rapidly [17, 18]. The most likely reason for the rapid variations in refractive index and other material parameters is the photoinduced transformation of defect centres in the germanosilicate glass network [19].

Figure 8 plots $(d\Omega/d\varepsilon)^0_{Ph}$ against germanium concentration in the core for FBGs written in different fibres (Table 1) at low UV fluences ($(d\Omega/d\varepsilon)^0_{Ph}$ was evaluated using relations (10) and (11)). The linear behaviour of the data lends support to the above conclusion as to the role of defect centres in the glass network. In particular, the concentration of GeE' defects forming in germanosilicate glass at low UV fluences is proportional to the germanium concentration [20, 21].

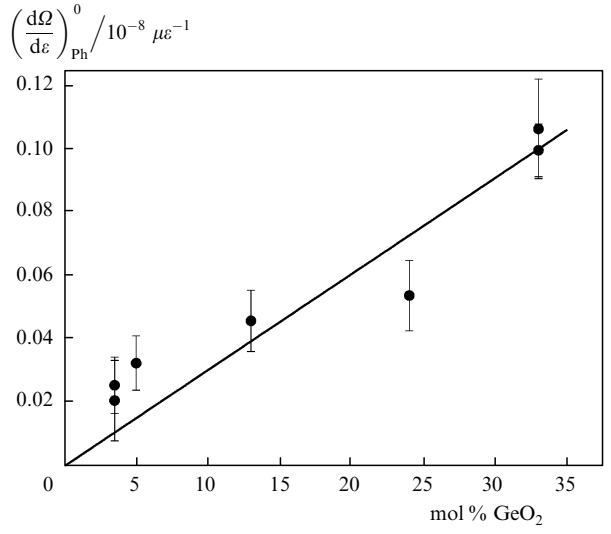

Figure 8. $(d\Omega/d\varepsilon)^0_{Ph}$ vs. germanium concentration in the fibre core for FBGs written with low UV fluences.

After a rapid variation at low fluences, $d\Omega/d\varepsilon$ and $d\Omega/dT$ grow monotonically (Fig. 7) even though the photoinduced index change in the FBGs under consideration is a more intricate function of fluence, as represented by (17). The second stage of the growth of $d\Omega/d\varepsilon$ and $d\Omega/dT$ correlates well with the fluence dependence of the population of level 3, corresponding to type IIa photosensitivity (Fig. 7, solid line). This leads us to assume that both temperature- and strain-induced reversible changes in Ω (and hence in the reflectivity of the FBG) in this region are dominated by type IIa photosensitivity.

6. Conclusions

The present results on strain- and temperature-induced reversible changes in the reflectivity of FBGs led us to a number of conclusions that, in our opinion, provide additional information important for understanding the microscopic mechanisms of photoinduced index changes in optical fibres.

In particular, our results show that, the strain and temperature effects on the reflectivity of the FBGs written after low-temperature hydrogen loading of the fibre are relatively weak and can be accounted for in terms of reversible changes in the guidance characteristics of the fibre and parameters of the FBGs under the assumption that parameters of the germanosilicate glass are unaffected by the UV exposure.

The reversible changes in the reflectivity of the FBGs written in unloaded fibres have a markedly different character. In particular, such changes in the type I and IIa gratings are almost an order of magnitude greater than those in the type I(H_2) FBGs, which can be understood in terms of photoinduced changes in parameters of the core glass (p_{12} and dn/dT). Note that the opposite signs of the observed reversible changes in R_{Br} in the type I and IIa FBGs are due to the opposite signs of the photoinduced index changes in these gratings.

Analysis of reversible changes in R_{Br} in relation to the UV fluence indicates that such changes are significant even at low fluences (1 kJ cm^{-2}). The initial increase $d\Omega/d\varepsilon$ and $d\Omega/dT$ in the type I and IIa FBGs is proportional to the increase in the germanium content of the fibre core. The present data suggest that the reversible changes at low fluences are due to photoinduced transformations of defect centres in the germanosilicate glass network.

With increasing UV fluence (>1 kJ cm^{-2}), both $d\Omega/d\varepsilon$ and $d\Omega/dT$ increase monotonically (whereas Ω is a non-monotonic function of fluence), which correlates well with the increase in the population of state 3 in the model proposed by Dong et al. [12]. This suggests that the physical mechanism behind type IIa photosensitivity (photoinduced bond breaking in the glass network [22]) influences the elasto-optic and thermo-optic coefficients of the germanosilicate glass. At the same time, the present results demonstrate that the photoinduced densification of the glass network (type I photosensitivity [23]) has little effect on these coefficients.

An important point is that the present experimental results show that the strain- and temperature-induced reversible changes in the reflectivity of FBGs have a general character.

References

1. Kashyap R. *Fiber Bragg Gratings* (San Diego, CA: Acad. Press, 1999).
2. Othonos A., Kalli K. *Fiber Bragg Gratings: Fundamentals and Applications in Telecommunications and Sensing* (Norwood, Mass.: Artech House, 1999).
3. Vasil'ev S.A., Medvedkov O.I., Korolev I.G., Bozhkov A.S., Kurkov A.S., Dianov E.M. *Kvantovaya Elektron.*, **35**, 1085 (2005) [*Quantum Electron.*, **35**, 1085 (2005)].
4. Erdogan T., Mizrahi V., Lemaire P.J., Monroe D. *J. Appl. Phys.*, **76**, 73 (1994).
5. Iocco A., Limberger H.G., Salathe R.P., Everall L.A., Chisholm K.E., Williams J.A.R., Bennion I. *IEEE J. Lightwave Technol.*, **17**, 1217 (1999).
6. Kersey A.D., Davis M.A., Patrick H.J., LeBlanc M., Koo K.P., Askins C.G., Putnam M.A., Friebele E.J. *IEEE J. Lightwave Technol.*, **15**, 1442 (1997).
7. Shu D., Zhao X., Zhang L., Bennion I. *Appl. Opt.*, **43**, 2006 (2004).
8. Hidayat A., Wang Q., Niay P., Douay M., Poumellec B., Kherboushe F., Riant I. *Appl. Opt.*, **40**, 2632 (2001).
9. Akulov V.A., Afanasiev D.M., Babin S.A. Churkin D.V., Kablukov S.I., Rybakov M.A., Vlasov A.A. *Laser Phys.*, **17**, 124 (2007).
10. Vlasov A.A. *Cand. Sci. Diss.* (Novosibirsk: Inst. of Automation and Electrometry, Siberian Branch, Russ. Acad. Sci., 2009).

11. Medvedkov O.I., Korolev I.G., Vasil'ev S.A. Preprint No 6 (Moscow: Nauchn. Tsentr Volokonnoi Optiki, Inst. Obshchei Fiziki Ross. Akad Nauk, 2004).
12. Dong L., Liu W.F., Reekie L. *Opt. Lett*., **21**, 2032 (1996).
13. Gianino P.D., Bendow B. *Appl. Opt.,* **20**, 430 (1981).
14. Aashira R., Madhav K.V., Ramamurty U., Asokan S. *Opt. Lett.,* **34**, 2414 (2009).
15. Bozhkov A.S., Vasil'ev S.A., Medvedkov O.I., Grekov M.V., Korolev I.G. *Prib. Tekh. Eksp*., **4**, 76 (2005).
16. Dong L., Liu W. F. *Appl. Opt*., **36**, 8222 (1997).
17. Flockhart G.M.H., Cranch G.A., Kirkendall C.K. *Appl. Opt*., **46**, 8237 (2007).
18. Williams G.M., Putnam M.A., Tsai T.E., Askins C.G., Friebele E. J. *Proc. Techn. Dig. BGPP* (Washington, 1995) p. SuA5/82.
19. Neustruev V.B. *J. Phys.: Condens. Matter*, **6**, 6901 (1994).
20. Dong L., Archambault J.L., Reekie L., Russel P.S.J., Payne D.N. *Appl. Opt*., **34**, 3436 (1995).
21. Dong L., Pinkstone J., Russell P.S.J., Payne D.N. *J. Opt. Soc. Am. B,* **11**, 2106 (1994).
22. Kukushkin S.A., Shlyagin M.G., Swart P.L., Chtcherbakov A.A., Osipov A.V. *J. Appl. Phys*., **102**, 053502 (2007).
23. Poumellec B., Guenot P., Riant I., Sansonetti P., Niay P., Bernage P., Bayon J.F. *Opt. Mater*., **4**, 441 (1995).